NASA TECHNICAL MEMORANDUM

NASA TM X-3127

NASA TM X-3127



# MODIFICATIONS THAT IMPROVE PERFORMANCE OF A DOUBLE ANNULAR COMBUSTOR AT SIMULATED ENGINE IDLE CONDITIONS

*Donald F. Schultz*

*Lewis Research Center*

*Cleveland, Ohio 44135*

NATIONAL AERONAUTICS AND SPACE ADMINISTRATION • WASHINGTON, D. C. • DECEMBER 1974

| 1. Report No. NASA TM X-3127 | 2. Government Accession No. | 3. Recipient's Catalog No. |
|---|---|---|
| 4. Title and Subtitle MODIFICATIONS THAT IMPROVE PERFORMANCE OF A DOUBLE ANNULAR COMBUSTOR AT SIMULATED ENGINE IDLE CONDITIONS | | 5. Report Date December 1974<br>6. Performing Organization Code |
| 7. Author(s) by Donald F. Schultz | | 8. Performing Organization Report No. E-7960<br>10. Work Unit No. 501-24 |
| 9. Performing Organization Name and Address Lewis Research Center<br>National Aeronautics and Space Administration<br>Cleveland, Ohio 44135 | | 11. Contract or Grant No.<br>13. Type of Report and Period Covered Technical Memorandum |
| 12. Sponsoring Agency Name and Address National Aeronautics and Space Administration<br>Washington, D. C. 20546 | | 14. Sponsoring Agency Code |
| 15. Supplementary Notes | | |

16. Abstract

Three techniques were evaluated to determine if simple combustor modifications could be used to reduce the engine ground idle emissions of a double annular combustor designed for Mach 3.0 cruise operation. These techniques were radial fuel staging, the use of radial-inflow rather than axial-flow air swirlers, and the optimization of fuel-nozzle spray angle and differential pressure. Radial fuel staging and the use of radial-inflow air swirlers significantly improved performance at two ground idle test conditions simulating both low- and high-compression ratio engines.

| 17. Key Words (Suggested by Author(s)) | 18. Distribution Statement |
|---|---|
| Jet engine; Combustors (double annular); Combustion efficiency; Air pollution; Exhaust gases; Combustion; Idle condition | Unclassified - unlimited<br>Category 33 |

| 19. Security Classif. (of this report) | 20. Security Classif. (of this page) | 21. No. of Pages | 22. Price* |
|---|---|---|---|
| Unclassified | Unclassified | 30 | $3.25 |

* For sale by the National Technical Information Service, Springfield, Virginia 22151

# MODIFICATIONS THAT IMPROVE PERFORMANCE OF A DOUBLE ANNULAR COMBUSTOR AT SIMULATED ENGINE IDLE CONDITIONS

by Donald F. Schultz

Lewis Research Center

## SUMMARY

A testing program was undertaken to determine if the emissions of an idling engine could be reduced by making simple combustor modifications. Three techniques were tested: radial fuel staging, the use of radial-inflow instead of axial-flow air swirlers, and the optimization of fuel-nozzle spray angle and differential pressure. A double-annular ram-induction combustor designed for Mach 3.0 cruise was used for these tests. Two test conditions, simulating ground idle conditions for both low- and high-compression ratio engines, were used.

Two significant results were obtained: (1) Combustion efficiency at both the low and high idle conditions was significantly higher with radial fuel staging than with combustion in both annuli. This improved efficiency caused a considerable decrease in the levels of idle emissions. (2) Radial-inflow air swirlers performed much better than axial-flow swirlers, allowing stable operation at some low idle points where combustion could not be maintained using axial-flow swirlers.

## INTRODUCTION

An investigation was conducted to determine what improvements in exhaust emissions might be effected by relatively simple modifications to a gas turbine engine combustor. Two primary pollution exhaust emissions exist at ground idle: unburned hydrocarbons and carbon monoxide. Oxides of nitrogen, the primary pollution emission at takeoff and cruise, is normally a secondary emission problem at idle.

Engine cycle has a significant effect on ground idle emissions. To meet the 1979 Environmental Protection Agency emissions standards (ref. 1) for hydrocarbons and carbon monoxide, a 99 percent combustion efficiency is required at idle. Therefore, a high-compression-ratio engine, with its higher inlet-air temperature and pressure and resulting higher combustion efficiency at idle, has a significant advantage over a low-compression-ratio engine in attempting to meet this standard. The high-compression-ratio engine, however, has a much greater oxides of nitrogen emission problem at takeoff and cruise than does low-compression-ratio engine.

At ground idle many low-compression-ratio engines have combustion efficiencies as low as 60 percent, whereas most high-compression engines have about 90 percent combustion efficiency at ground idle.

In this program several simple approaches were studied to determine by how much ground-idle emissions could be reduced. The main effort is aimed at raising combustion efficiency. A comparison was made of the effects of axial-flow and radial-inflow air swirlers on combustion efficiency due to the significant differences at the air-fuel interface between the two methods. Radial fuel staging was suggested because increasing fuel-nozzle pressure differential and increasing fuel-air ratio both tend to increase combustion efficiency. Radial fuel staging permits twice the fuel flow in a burning annulus for the same overall temperature rise compared with combustion in both annuli. Radial staging also eliminates the adverse stress effects of combustion in combustor sectors that leave alternately hot and cold sectors in the combustor exit and turbine planes. Fuel-nozzle spray angle and fuel-nozzle differential pressure effects were studied to determine the magnitude of the second-order improvements in combustion efficiency that might be obtained by optimizing them. Additional information on fuel injection techniques is given in reference 2, which gives data on a $90^{\circ}$ sector test of a double-annular combustor using air assist and air blast fuel nozzles and compares their performances with each other and with simplex fuel nozzles.

The combustor used for these tests was a double-annular combustor designed for a large turbofan engine operating at flight speeds up to Mach 3.0 cruise. Two simulated engine ground idle conditions were chosen for testing to demonstrate these effects on both low- and high-pressure-ratio engines.

Combustion efficiency was determined by both gas analysis and thermocouple measurement. Data will be provided to show the effects of the described modifica-

tions on the exhaust emission of unburned hydrocarbons, carbon monoxide, and oxides of nitrogen and their effects on exit temperature profiles, pressure loss, and combustion efficiency. The investigation was conducted in a full-scale engine component, connected-duct research facility at Lewis. The two test conditions have a common reference velocity of 32 meters per second and a fuel-air ratio range of 0.008 to 0.012. One condition has an inlet temperature of 367 K and an inlet total pressure of 20.2 newtons per square centimeter simulating a low-pressure-ratio engine; the other condition has an inlet air temperature of 478 K and an inlet total pressure of 40.5 newtons per square centimeter simulating a high-pressure-ratio engine. Ideal combustor temperature rises vary from 290 to 470 K over the fuel-air ratio range to be tested.

Appendixes A and B give details concerning combustor design and instrumentation, and appendixes C and D contain the calculations and the definitions of the symbols. Additional calculations and test facility details are given in reference 3.

## APPARATUS

### Combustor Description

This investigation was conducted using a double-annular, ram-induction combustor designed for Mach 3.0 cruise. Figure 1 shows a cross section of the combustor. A description of this combustor is given in appendix A.

### Air Swirler Description

The radial-inflow and axial-flow air swirlers used in these tests are shown in figure 2. Figure 3 shows the airflow versus differential pressure for both swirlers. The swirler differential pressure was about 0.39 newton per square centimeter at both the low and high idle test conditions. At this differential pressure both types of swirler flow about the same amount of air at the same inlet pressure. It should be noted that the data of figure 3 resulted from a calibration test made at ambient discharge pressure with ambient temperature air. Therefore, these airflows must be corrected for temperature and pressure when determining the exact swirler airflows at the various test conditions.

## Fuel Nozzle Description

Five sets of simplex fuel nozzles were used for these tests. Fuel nozzle spray angles of $60^{\circ}$, $80^{\circ}$, and $90^{\circ}$ were evaluated. Table I summarizes the fuel flow characteristics for all the fuel nozzles used. All fuel nozzles were flow checked to ensure their flow was within 2 percent of their nominal value at their design flow pressure.

## Comparison of Radial-Inflow and Axial-Flow Air Swirlers

Figure 4 is a comparison of radial-inflow and axial-flow air swirlers showing combustion efficiency at various fuel-air ratios at the low and high idle conditions. This figure shows that the radial-inflow air swirlers were far superior to the axial-flow swirlers although both types flow the same amount of air. Using the axial-flow swirlers, ignition could not be obtained or combustion could not be maintained at many low idle points. With radial-inflow swirlers, ignition and combustion were obtained at all test points. As expected, combustion efficiency increased with increasing fuel-air ratio at both low and high idle. Because of the superior performance of the radial-inflow swirlers, they were used in the remaining tests reported herein.

## TEST CONDITIONS

Two test conditions were chosen to be representative of idle conditions for low- and high-pressure-ratio subsonic and supersonic fan engines. These conditions will be referred to as low and high idle and are defined in table II. Fuel-air ratios ranged from 0.008 to 0.012 to broaden the applicability of the data. Fuel-air ratio is defined as total fuel flow injected divided by total airflow to the combustor. In the case of radial fuel staging (fuel flow to only one of the two combustor annuli), the same fuel flow that is supplied to both annuli at a given fuel-air ratio is then supplied to only one annulus. Thus, the local fuel-air ratio is double the overall fuel-air ratio. Reference 3 gives details of the test facility and its operation. Appendix B discusses the instrumentation used during these tests including the gas analysis equipment.

## RESULTS

Table III is a list of test results for the low and high idle conditions. ASTM Jet A fuel was used for all tests. Some figures show data at zero combustion efficiency. These points indicate that blowout occurred and no ignition could be obtained at that condition. No effort was made to improve the exit-temperature distribution. Table IV shows performance at simulated takeoff and Mach 2.7 and 3.0 cruise with this combustor for reference. The double figures under the "fuel-nozzle differential pressure" column represent the fuel nozzle differential pressure in each annulus (inner annulus, outer annulus). Both numbers are given as partial radial fuel staging was used to improve the exit-temperature profile factor.

A FARR value (defined in appendix C) was used to determine gas analysis data quality. An ideal FARR value is 1.0. All data that deviated by greater than 5 percent are marked by a flag.

### Effects of Radial Fuel Staging

At idle operation, due to the low heat release rates, it is practical to operate the combustor while supplying fuel to only one annulus. Figure 5 compares the maximum exit temperatures encountered at low and high idle over the range of fuel-air ratios tested using radial fuel staging. The figure indicates that maximum exit temperatures of 1095 and 1355 K for low and high idle, respectively, were obtained. These maximum temperatures were obtained while supplying fuel to the inner annulus. This was also the fuel staging configuration that gave the highest combustion efficiency. For comparison the maximum temperatures at takeoff and Mach 3.0 cruise for this combustor are 1829 and 1564 K, respectively.

The maximum average radial temperatures encountered at low and high idle over the range of fuel-air ratios tested, while using radial fuel staging, were 1006 and 1182 K, respectively, for low and high idle. These temperatures occurred with fuel supplied to only the inner annulus. With fuel supplied to the outer annulus only maximum average radial temperatures were somewhat lower, which reflected somewhat lower combustion efficiency. These numbers compare with 1507 and 1501 K for takeoff and Mach 3.0 cruise, respectively.

Combustion efficiency and emissions. - Combustion efficiency can be increased significantly by use of radial fuel staging. This increase is most dramatic at the low idle condition and at the lower fuel-air ratios at both idle conditions. Figure 6 shows the increases in combustion efficiency that are obtainable with radial fuel staging. At low idle, with a fuel-air ratio of 0.008, the combustion efficiency increased from 47 to 69.5 percent when fuel was supplied to the inner annulus only as compared to supplying the same total fuel flow to both annuli. Part of this increase in combustion efficiency (perhaps 5 percentage points) is due to increased fuel-nozzle differential pressure, which gives better atomization of the fuel. A discussion of this effect appears later. The remainder of the improvement is due to better burning from a richer fuel mixture.

Figure 6 also shows that at high idle combustion efficiency is higher with radial fuel staging, but the difference in combustion efficiency between fuel flow in only the inner or only the outer annuli is negligible. At an overall fuel-air ratio of 0.008, combustion efficiency increased from 90 to 96 percent when radial fuel staging was employed. Combustion efficiency also increased from 90 to 95.5 percent when the fuel-air ratio was increased from 0.008 to 0.012 with fuel supplied to both annuli.

A 2-percentage-point increase in combustion efficiency was observed when the fuel-air ratio was increased over the same range with radial fuel staging (96 to 98 percent).

Emission indices for hydrocarbons and carbon monoxide are shown only for the high idle condition because of the low combustion efficiencies encountered at low idle. The hydrocarbon and carbon monoxide data at the high idle condition are shown in figure 7. Figure 7(a) indicates that radial fuel staging can give a fourfold reduction in hydrocarbons emissions at a 0.008 fuel-air ratio; an emission index of 69 grams per kilogram of fuel for combustion in both annuli is reduced to 16 grams per kilogram of fuel for combustion in the inner annulus only. In like manner carbon monoxide emissions decreased from 130 to 78 grams per kilogram of fuel (fig. 7(b)). Both hydrocarbons and carbon monoxide indices decreased considerably with increasing fuel-air ratio. The hydrocarbon emission index decreased from 16 to 7.5 grams per kilogram of fuel with combustion in the inner annulus only when the fuel-air ratio was increased from 0.008 to 0.012. In like manner the carbon monoxide emission index decreased from 78 to 59 grams per kilogram of fuel with the same fuel-air ratio change.

Figure 7(c) shows the variation in the oxides of nitrogen ($NO_x$) emission index at various fuel-air ratios and the effect of radial fuel staging at high idle. This figure shows that $NO_x$ emission index can nearly double when combustion is sustained in only one annulus. However, the maximum value of $NO_x$ emission index is still a relatively low, 1.8 grams per kilogram of fuel. At low idle $NO_x$ emission index increased only about 40 percent with radial fuel staging. Its value was nearly constant over the fuel-air ratio tested and never exceeded 1.0 gram per kilogram of fuel. This lower $NO_x$ value at low idle is due primarily to inlet-temperature and pressure effects on $NO_x$ formation as well as the lower value of combustion efficiency.

Radial temperature profile. - Figure 8 shows the radial average temperature profile present with radial fuel staging for the high idle condition. Examination of this figure shows there is little difference in profile severity between combustion in only inner annulus or only the outer annulus. Figure 6 indicates that combustion efficiency in both cases was 98.0 percent. Of course, the temperature profile is least severe with combustion in both annuli; however, the combustion efficiency was only 95.4 percent in that case.

Total pressure loss. - Radial fuel staging had no measurable effect on total-pressure loss. Total-pressure loss was 7.2 percent at high idle (diffuser-inlet Mach number, 0.281) and 9.8 percent at low idle (diffuser-inlet Mach number, 0.322).

## Optimum Fuel-Nozzle Spray Angle

Fuel nozzles with $60^\circ$, $80^\circ$, and $90^\circ$ spray angles were evaluated at the two idle conditions to determine the effect of spray angle on idle performance. Figure 9 shows combustion efficiency as a function of fuel-nozzle spray angle at various fuel-air ratios for the low idle condition. In addition, radial fuel staging with combustion only in the inner annulus was used. Data obtained without radial fuel staging and with fuel flow only to the outer annulus gave similar results.

An examination of figure 9 shows that the highest combustion efficiency is obtained with a fuel-nozzle spray angle of about $80^\circ$. Unburned hydrocarbons, as expected, reached minimum values at points where combustion efficiency peaked. Carbon monoxide emissions index increased with increasing fuel-nozzle spray angle at low idle from an emissions index of 175 grams per kilogram of fuel at $60^\circ$ spray angle to 250 grams per kilogram of fuel at $90^\circ$ spray angle, but decreased slightly from

85 grams per kilogram of fuel at 60° spray angle to 80 grams per kilogram of fuel at 90° spray angle at high idle. In both cases combustion was in the inner annulus only at a fuel-air ratio of 0.008. Thus a spray angle of 60° gave a minimum carbon monoxide emissions index at low idle, and a spray angle of 90° gave a minimum carbon monoxide emissions index at high idle. However, at high idle the difference in carbon monoxide emissions index at 80° and 90° fuel-nozzle spray angle is negligible. Thus, an 80° fuel-nozzle spray angle seems to be optimum in nearly all respects. It was also found that the $NO_x$ emission index minimized at an 80° spray angle at the high idle condition but maximized at 80° spray angle at low idle. In both cases, however, the $NO_x$ emission index is low, reaching a maximum of 1.68 grams per kilogram of fuel at high idle and 1.05 grams per kilogram of fuel at low idle with a spray angle of 80°.

### Effect of Fuel Nozzle Differential Pressure

At the low and high idle conditions combustion efficiency increased with increasing fuel nozzle differential pressure over the entire fuel differential pressure range tested (12 to 755 $N/cm^2$). Three sizes of fuel nozzles at the same spray angle were tested. At low idle with a fuel-air ratio of 0.012 and a combustion in both annuli, combustion efficiency increased from 8 to 62 percent as fuel-nozzle differential pressure was increased from 10 to 300 newtons per square centimeter. However, little improvement in combustion efficiency is gained at fuel-nozzle differential pressures greater than 350 newtons per square centimeter.

## DISCUSSION

### Comparison of Radial-Inflow and Axial-Flow Swirlers

The significant improvement in performance of the radial-inflow swirlers over that of the axial-flow swirlers is most likely a result of the immediate contact of the fuel with the turbulent swirled air as it leaves the fuel nozzle. In the case of axial-flow swirlers, the fuel traveled perhaps 6 or 7 millimeters before coming into contact with the turbulent air stream. This delay in contact with the turbulent air stream allowed carbon to build up on the fuel nozzle face. This carbon buildup occasion-

ally caused fuel streaking, which ended after a few minutes when the carbon broke loose. This occasional fuel streaking sometimes caused the pattern factors to nearly double. This problem was never encountered with the radial-inflow swirlers. Perhaps a different design for the axial-flow swirlers would overcome their short comings.

## Radial Fuel Staging

The EPA standards translate approximately into an emission index of 20 grams per kilogram of fuel for carbon monoxide and 4 grams per kilogram of fuel for unburned hydrocarbons. The best results with radial fuel staging in this combustor indicate emissions indices of 59 and 7.5 grams per kilogram of fuel for carbon monoxide and unburned hydrocarbons, respectively, at the high idle conditions. These values were obtained with a moderate fuel nozzle differential pressure of 124 newtons per square centimeter. A serious problem with the double-annular combustor design in this size (outer shroud diameter, 94 cm) is the relatively narrow annulus heights of 55 and 65 millimeters for the outer and inner annuli, respectively. The performance was equal or better in all cases with combustion in the wider inner annulus than in the outer annulus. In all likelihood, as combustor diameter is increased, combustion efficiency will increase as well. Air assist and air blast fuel nozzles (ref. 2) are other alternatives that could help combustors such as a double annular combustor meet the EPA standards at least at the high idle condition.

It is obvious that there is little hope of reducing the low-idle-condition emissions enough for this combustor to meet the EPA standards. It is extremely difficult for any combustor design to perform adequately in a low-compression-ratio engine of this size because of the low combustor-inlet-air temperature and pressure and the low exit-temperatures involved.

## Fuel-Nozzle Spray Angle

Fuel-nozzle spray angle, though a secondary effect, did have a small influence on combustion efficiency at the low idle condition. Fuel-nozzle spray angle could likely be used to trim an engine into specification that nearly meets the EPA standards since carbon monoxide emissions index was inversely proportional to fuel-

nozzle spray angle and unburned hydrocarbons tended to minimize at an $80^{\circ}$ spray angle.

### Fuel-Nozzle Differential Pressure

Combustion efficiency tends to increase with increasing fuel-nozzle differential pressure. This increase results from the fact that increasing pressure decreases fuel droplet size, thus causing the fuel to vaporize and burn faster. As inlet-air temperature increases, the improvement in combustion efficiency is minimized for increased fuel pressure because the inlet-air temperature becomes a more significant factor in fuel vaporization than fuel atomization. Also, the smaller the fuel droplets, the less chance they have of contacting the combustor liner before they are burned. Thus, combustion efficiency is increased because the burning droplets are not quenched by coming into contact with the liner walls. There is evidence that oxides of nitrogen may either increase or decrease with increasing fuel nozzle differential pressure. This increase or decrease is a second-order effect that is apparently a function of primary-zone fuel-air ratio.

## SUMMARY OF RESULTS

Full-scale tests were conducted on a short, double-annular, ram-induction combustor to determine the effects on combustor performance at ground idle of relatively simple modifications to an engine combustor that could reduce exhaust emissions during idle. Four concepts were tested at conditions simulating both a low- and a high-pressure-ratio engine.

The following results were obtained in this study:

1. Radial-inflow air swirlers were superior to axial-flow swirlers. At many of the test points obtained with radial-inflow swirlers, combustion could not even be maintained with axial-flow swirlers.

2. Radial fuel staging gave a fourfold reduction in hydrocarbon emissions at a 0.008 fuel-air ratio, at the high idle condition. Both carbon monoxide and hydrocarbon emissions indices decreased significantly with increasing fuel-air ratio.

3. Combustion efficiency increased significantly with radial fuel staging over that for combustion in both annuli. The greatest increases in combustion efficiency

occurred with combustion in the inner annulus only.

4. The oxides of nitrogen emissions index increased when radial fuel staging was used.

5. Radial average exit temperatures reached acceptable values of 1006 and 1182 K at low and high idle, respectively, and the maximum radial exit temperatures reached acceptable values of 1095 and 1355 K for the low and high idle conditions, respectively, when combustion was maintained in only one annulus at an overall fuel-air ratio of 0.012.

Lewis Research Center,
National Aeronautics and Space Administration,
Cleveland, Ohio, July 25, 1974,
501-24.

# APPENDIX A

# COMBUSTOR DESIGN

## The Double-Annular Concept

The combustor used in this investigation is a double-annular ram-induction combustor. The ram-induction concept of combustor construction is discussed in references 3 and 4. Constructing the combustion zone as a double annulus permits a shorter combustor while maintaining an adequate ratio of length to annulus height in each combustion zone. The individual control of the inner and outer annulus fuel systems of the double-annular combustion zone provides a useful method for adjusting the outlet radial temperature profile. This individual fuel control can be extended to include radial fuel staging, which is useful at engine idle conditions.

## Combustor Design Details

The double-annular, ram-induction combustor including the diffuser section used for this investigation is shown in cross section in figure 1. Forward airflow spreaders in the diffuser split the inlet airflow into three passages leading into the combustor. These are the inner liner passage, the outer liner passage, and the center passage. About 50 percent of the airflow is ducted by shrouds surrounding the outside of both the outer and inner liners of the combustors. The high velocity airflow which is maintained from the diffuser inlet through this ducting is turned into the combustor burning zones by means of the scoops. The first row of scoops supplies air to the primary zone, and the second row supplies diluent air to the secondary zone.

Basic dimensions for this combustor are shown in figure 1. The diameters are essentially those of the combustor for the Pratt & Whitney Aircraft experimental supersonic transport engine (JTF 17 (ref. 4)). However, the diffuser-combustor overall length of the double-annular combustor is about 30 percent shorter than that used in the JTF 17 engine.

Photographs of the combustor are shown in figure 10. Figure 10(a) shows the downstream end with the two circumferential rows of scoops of the inner and outer liners and those of the center section. Figure 10(b) is a closeup of this same view showing more detail of the scoop arrangement. The fuel nozzles and associated

swirlers are removed, but the deflectors for cooling the inner and outer headplates are shown at the nozzle locations. A side view of the combustor with the upstream diffuser airflow spreaders and inner exit transition liner added to the combustor is shown in figure 10(c). The notches in the airflow spreaders fit around the diffuser struts. The combustor is pin mounted through the struts using tangs attached to the inner and outer headplates that extend forward into the airflow spreaders.

The major items in the combustor design are listed in table V. The circumferential locations of combustor components such as scoops, fuel nozzles, and diffuser struts are shown in figure 11. The flow areas as distributed among the many openings (scoops, film cooling, swirlers, etc.) are given on the combustor sketch of figure 12. The scoop discharge areas with length and width dimensions are listed in table VI.

## APPENDIX B

## INSTRUMENTATION

### Measurement Methods

Measurements to determine combustor operating and performance were recorded by the Lewis central automatic data processing system (ref. 5). Control room readout instrumentation (indicating and recording) was used to set and monitor the test conditions and the operation of the combustor. Pressures were measured and recorded by the central digital automatic multiple pressure recorder (DAMPR) and by strain-gage pressure transducers (ref. 6). Iron-constantan thermocouples were used to measure temperatures between 140 to 675 K, Chromel/Alumel thermocouples measured temperatures between 240 and 1560 K. High temperatures, 275 to 1920 K were measured with platinum-13 percent-rhodium/platinum thermocouples. The indicated readings of all thermocouples were taken as true values of the total temperatures. The platinum-13 percent-rhodium/platinum thermocouples were of the high-recovery aspirating type (ref. 7, type 6).

Airflow rates were measured by square-edged orifices installed according to ASME specifications. Fuel flow rates were measured by turbine flowmeters using frequency-to-voltage converters for readout and recording.

### Instrumentation Stations

The locations of the combustor instrumentation stations are shown in figure 1. Inlet-air temperature was measured by eight Chromel/Alumel thermocouples that were equally spaced around the inlet while inlet air total pressure was measured by eight five-point total pressure rakes. The pressure rakes measured the total pressure profile at centers of equal areas across the inlet annulus. Static pressure at the inlet was measured by 16 wall static pressure taps with 8 on the outer and 8 on the inner walls of the annulus at station 3.

Combustor-outlet total temperature and pressure at instrumentation station 4 were measured at $3^{\circ}$ increments around the exit circumference. At each measurement location, five temperature and pressure points were measured across the annulus.

The water-cooled probe assembly contained five temperature and pressure sensors. A detail of this probe is shown in reference 3. Those areas of these probes that were exposed to the hot exhaust gases were made of a platinum-rhodium alloy. Also located at station 4 were eight wall static pressure taps.

## APPENDIX C

## CALCULATIONS

This appendix provides information on the computation of combustion efficiency by thermocouple measurement and by exhaust gas analysis. Combustion efficiency computed by thermocouple measurement was used only when the combustion efficiency computed by gas analysis was less than 75 percent. Reference 3 details the computations of reference velocity, diffuser-inlet Mach number, total-pressure loss, and exit-temperature profile parameters of pattern factor, stator factor, and rotor factor.

### Combustion Efficiency by Thermocouple Measurement

Efficiency by thermocouple measurement was determined by dividing the measured temperature rise across the combustor by the theoretical temperature rise. The theoretical rise is calculated from the fuel-air ratio, fuel properties, inlet-air temperature and pressure, and the amount of water vapor present in the inlet airflow. The exit temperatures were measured with five-point traversing aspirated thermocouple probes and were mass-weighted for the efficiency calculation. The indicated readings of all thermocouples were taken as true values of the total temperatures. The mass-weighting procedure is given in reference 4. In each mass-weighted average, 585 individual exit temperatures were used.

### Combustion Efficiency by Gas Analysis and Sample Validity

Efficiency by gas analysis was determined by measuring the exhaust products of carbon dioxide, carbon monoxide, and unburned hydrocarbons. The derived combustion efficiency was validated by determining the combustor fuel-air ratio from the exhaust analysis. This fuel-air ratio was compared with the metered fuel-air ratio by dividing the metered ratio value into the gas analysis ratio value. This fuel-air ratio ratio, FARR in the data (table III) is defined as:

$$FARR = \frac{\text{Fuel/Air (gas analysis)}}{\text{Fuel/Air (metered)}}$$

FARR values of 1.0±0.05 were considered acceptable. Nearly all data fall in this range.

## Units

The U.S. Customary system of units was used for primary measurements and calculations. Conversion to SI units (Système International d'Unités) is done for reporting purposes only. In making the conversion, consideration is given to implied accuracy and may result in rounding off the values expressed in SI units.

## REFERENCES


1. Control of Air Pollution from Aircraft Engines - Emissions Standards and Test Procedures for Aircraft. Federal Register, vol. 38, no. 136, July 17, 1973.

2. Clements, T. R.: Effect of Fuel Zoning and Fuel Nozzle Design on Pollution Emissions at Ground Idle Conditions for a Double-Annular Ram-Induction Combustor. PWA-FR-5295, Pratt & Whitney Aircraft (NASA CR-121094), 1973.

3. Schultz, Donald F.; and Perkins, Porter J.: Effects of Radial and Circumferential Inlet Velocity Profile Distortions on Performance of a Short-Length Double-Annular Ram-Induction Combustor. NASA TN D-6706, 1972.

4. Rusnak, J. P.; and Shaodwen, J. H.: Development of an Advanced Annular Combustor. PWA-FR-2832, Pratt & Whitney Aircraft (NASA CR-72453), 1969.

5. Staff of the Lewis Laboratory: Central Automatic Data Processing System. NACA TN 4212, 1958.

6. Mealey, Charles; and Kee, Leslie: A Computer-Controlled Central Digital Data Acquistion System. NASA TN D-3904, 1967.

7. Glawe, George E.; Simmons, Frederick S.; and Stickney, Truman M.: Radiation and Recovery Corrections and Time Constants of Several Chromel-Alumel Thermocouple Probes in High-Temperature, High-Velocity Gas Streams. NACA TN 3766, 1956.

TABLE I. - FUEL NOZZLE CHARACTERISTICS

[Differential pressure, 103 $N/cm^2$; 64 nozzles.]

| Nozzle | Spray angle deg | Flow, kg/sec |
|---|---|---|
| H4 | 60 | 0.945 |
| H5 | 60 | .841 |
| H6 | 60 | .855 |
| H3 | 80 | .85 |
| H2 | 90 | .82 |

TABLE II. - TEST CONDITIONS - ENGINE IDLE

| Engine pressure ratio | Inlet air conditions | | | Reference velocity, m/sec | Fuel-air ratio range |
|---|---|---|---|---|---|
| | Total pressure $N/cm^2$ | Temperature, K | Flow rate, kg/sec | | |
| Low | 20.2 | 370 | 26.3 | 32.0 | 0.008-0.012 |
| High | 40.5 | 475 | 40.4 | 32.0 | 0.008-0.012 |

TABLE III. - SUMMARY OF TEST DATA

| Run | Model | Diffuser inlet | | Reference velocity, $V_{ref}$, m/sec | Air weight flow, $\dot{W}_a$, kg/sec | Annulus supplied with fuel | Fuel-air ratio, F/A | Combustion efficiency, $\eta_c$, percent (a) | Pattern factor $\overline{\delta}$ | Fuel temperature, $T_{fuel}$, K | Combustor total pressure loss, $\Delta P/P_3$, percent | Fuel nozzle differential pressure, $N/cm^2$ | Inlet Mach number, $M_3$ | Exhaust emission, g/kg fuel | | | Fuel-air ratio ratio, FARR | Type of swirler | Fuel nozzle angle, deg | Combustion efficiency, $\eta_{cc}$, percent (b) |
|---|---|---|---|---|---|---|---|---|---|---|---|---|---|---|---|---|---|---|---|
| | | Total pressure, $P_{T3}$, $N/cm^2$ | Temperature, $T_3$, K | | | | | | | | | | | Oxides of nitrogen | Hydrocarbons | Carbon monoxide | | | | |
| 844 | 10-RH5 | 20.29 | 370 | 31.94 | 26.22 | Inner | 0.008 | 66.3 | 1.303 | 292 | 9.58 | 25.8 | 0.324 | ----- | ----- | ----- | ----- | Radial | H5 | ---- |
| 845 | ↓ | 20.27 | 369 | 31.91 | 26.24 | Inner | .0101 | 72.2 | 1.266 | 292 | 9.52 | 38.8 | .324 | 0.38 | 141.9 | 188.5 | 0.90 | ↓ | 60 | 81.4 |
| 846 | | 20.15 | ↓ | 32.15 | 26.28 | Inner | .0121 | 77.6 | 1.269 | 291 | 9.78 | 56.3 | .326 | ----- | ----- | ----- | ----- | | ↓ | ---- |
| 847 | | 20.12 | | 32.23 | 26.33 | Both | .0081 | 39.3 | 1.002 | 292 | 9.45 | 7.17 | .327 | .32 | 103.8 | 177.5 | .84 | | | 85.5 |
| 848 | | 20.12 | | 32.19 | 26.29 | ↓ | .008 | 42.5 | .679 | 292 | 9.41 | 6.68 | .327 | ----- | ----- | ----- | ----- | | | ---- |
| 854 | | 41.02 | 474 | 31.41 | 40.58 | | .008 | 88.0 | .232 | 290 | 6.67 | 14.48 | .275 | 1.10 | 82.9 | 99.8 | 1.03 | | | 89.4 |
| 856 | | 40.56 | 475 | 31.91 | 40.66 | | .01 | 92.7 | .226 | 290 | 6.82 | 22.7 | .279 | 1.35 | 52.8 | 95.8 | 1.01 | | | 92.5 |
| 857 | ↓ | 40.97 | 476 | 31.57 | 40.57 | ↓ | .012 | 95.9 | .285 | 290 | 6.69 | 32.8 | .275 | 1.46 | 30.7 | 82.4 | 1.00 | | ↓ | 95.0 |
| 1023 | 10-RH2 | 20.00 | 369 | 32.71 | 26.50 | Inner | .0081 | 66.9 | 1.108 | 294 | 10.12 | 26.5 | .332 | .50 | 241.0 | 246.7 | 1.05 | | 90 | 70.1 |
| 1024 | ↓ | 20.02 | 369 | 32.65 | 26.46 | Inner | .0121 | 70.2 | 1.127 | 294 | 10.2 | 40.5 | .331 | .42 | 234.9 | 257.4 | 1.04 | | ↓ | 70.5 |
| 1025 | | 19.98 | 370 | 32.72 | 26.45 | Inner | .0121 | 72.1 | 1.132 | 294 | 10.36 | 59.4 | .332 | .37 | 223.1 | 232.7 | .95 | | | 72.2 |
| 1073 | 10-RH3 | 20.44 | 368 | 31.45 | 26.12 | Both | .0123 | 77.9 | .256 | 315 | 9.75 | 13.29 | .3180 | .62 | 194.9 | 211.6 | .99 | | 80 | 75.6 |
| 1075 | ↓ | 20.22 | 367 | 31.98 | 26.25 | Both | .0081 | 46.9 | .654 | 302 | 9.55 | 5.44 | .3242 | .72 | 423.1 | 184.7 | .96 | | ↓ | 53.4 |
| 1076 | | 20.32 | 367 | 31.71 | 26.16 | Both | .0102 | 58.5 | .460 | 299 | 9.58 | 8.77 | .3211 | .69 | 332.5 | 205.2 | .97 | | | 61.9 |
| 1078 | | 20.43 | 369 | 31.45 | 26.08 | Outer | .0081 | 62.6 | 1.189 | 298 | 9.38 | 23.38 | .3182 | .89 | 289.3 | 226.1 | 1.03 | | | 65.8 |
| 1079 | | 20.30 | 370 | 31.84 | 26.14 | ↓ | .0101 | 67.8 | 1.081 | 297 | 9.65 | 37.83 | .3220 | .84 | 242.2 | 232.7 | 1.00 | | | 70.3 |
| 1080 | | 20.35 | 370 | 31.74 | 26.13 | | .0101 | 67.7 | 1.114 | 297 | 9.64 | 37.78 | .3210 | .86 | 241.4 | 225.6 | .97 | | | 70.6 |
| 1081 | | 20.36 | 370 | 31.70 | 26.13 | ↓ | .0123 | 68.1 | 1.162 | 296 | 9.70 | 55.71 | .3207 | .79 | 216.6 | 275.3 | .95 | | | 73.1 |
| 1082 | | 20.28 | 369 | 31.78 | 26.19 | Inner | .0081 | 69.5 | 1.085 | ↓ | 9.65 | 21.78 | .3224 | 1.02 | 262.3 | 212.7 | .96 | | | 68.8 |
| 1085 | | 20.48 | 365 | 31.30 | 26.30 | Inner | .0101 | 74.5 | 1.104 | | 9.52 | 35.36 | .3182 | .98 | 223.4 | 223.7 | .97 | | | 72.4 |
| 1087 | | 20.33 | 364 | 31.53 | 26.35 | Inner | .0121 | 78.5 | .965 | ↓ | 9.85 | 51.97 | .3213 | .86 | 137.6 | 214.3 | .91 | | | 81.2 |
| 1089 | | 40.53 | 477 | 32.64 | 41.42 | Both | .0079 | 89.4 | .283 | 299 | 7.33 | 13.51 | .2863 | .71 | 68.8 | 130.0 | .99 | | | 90.1 |
| 1090 | | 40.39 | 479 | 32.26 | 40.64 | Both | .01 | 93.6 | .234 | 298 | 7.14 | 21.77 | .2817 | .94 | 42.1 | 116.3 | .98 | | | 93.1 |
| 1091 | | 40.49 | 477 | 32.03 | 40.62 | Both | .012 | 96.6 | .234 | 298 | 7.14 | 31.50 | .2802 | 1.18 | 23.4 | 98.3 | .96 | | | 95.4 |
| 1092 | | 40.16 | 477 | 32.41 | 40.75 | Inner | .0079 | 99.6 | .843 | 297 | 7.19 | 53.58 | .2839 | 1.29 | 16.0 | 78.1 | .98 | | | 96.6 |
| 1093 | ↓ | 40.49 | 477 | 32.00 | 40.56 | ↓ | .01 | 101.0 | .890 | 298 | 7.09 | 86.19 | .2799 | 1.47 | 9.1 | 68.3 | .95 | | | 97.5 |
| 1095 | 10-RH3 | 40.47 | 475 | 31.82 | 40.48 | | .0118 | 102.4 | .914 | 298 | 7.16 | 124.30 | .2791 | 1.67 | 7.5 | 59.3 | .95 | | | 97.9 |
| 1096 | ↓ | 40.32 | 478 | 32.16 | 40.53 | ↓ | .0101 | 100.8 | .903 | 299 | 7.20 | 88.53 | .2812 | 1.67 | 7.1 | 66.0 | .97 | | | 97.7 |
| 1097 | | 40.62 | ↓ | 31.86 | 40.45 | Outer | | 93.2 | .893 | 299 | 7.05 | 91.84 | .2784 | 1.62 | 10.7 | 71.4 | .98 | | | 97.3 |
| 1098 | | 40.33 | | 32.21 | 40.60 | Outer | .008 | 92.0 | .744 | 299 | 7.10 | 58.14 | .2817 | 1.56 | 19.4 | 86.2 | 1.01 | | | 96.0 |
| 1099 | | 40.41 | | 32.11 | 40.55 | Outer | .012 | 94.0 | .968 | 297 | 7.22 | 132.03 | .2808 | 1.83 | 7.2 | 64.4 | .95 | | ↓ | 97.8 |
| 1120 | | 19.93 | 365 | 32.00 | 26.13 | Both | .0081 | 37.5 | 1.057 | 296 | 9.16 | 4.48 | .324 | .36 | 482.8 | 137.1 | .87 | | 60 | 48.5 |
| 1121 | | 19.85 | 363 | 32.08 | 26.22 | ↓ | .0101 | 44.9 | 1.120 | 291 | 9.30 | 7.26 | .326 | .34 | 397.2 | 160.3 | .83 | | | 56.5 |
| 1126 | ↓ | 20.02 | 370 | 32.88 | 26.66 | | .0119 | 60.7 | .539 | 298 | 10.0 | 10.48 | .332 | .33 | 280.5 | 207.5 | .97 | | | 67.1 |
| 1260 | 10-AH6 | 20.07 | 377 | 33.14 | 26.41 | | .012 | 8.9 | 5.11 | 299 | 8.66 | 12.94 | .332 | ----- | ----- | ----- | ----- | Axial | | ---- |
| 1264 | ↓ | 39.95 | 478 | 32.04 | 39.97 | | .0081 | 72.7 | .535 | 298 | 6.29 | 14.27 | .279 | .315 | 215 | 215 | 1.004 | ↓ | | 74.9 |
| 1266 | | 39.79 | 475 | 32.25 | 40.38 | | .01 | 81.5 | .46 | 298 | 6.49 | 22.29 | .282 | .684 | 146 | 146 | .982 | | | 82.2 |
| 1267 | ↓ | 40.07 | 474 | 32.03 | 40.40 | ↓ | .012 | 88.7 | .51 | | 6.57 | 32.28 | .280 | .822 | 126 | 126 | .968 | ↓ | ↓ | 88.9 |

[a] By thermocouple measurement.
[b] By gas analysis.

TABLE IV. - PERFORMANCE AT SIMULATED TAKEOFF, MACH 2.7, AND 3.0 CRUISE OPERATION

[Fuel nozzle, H3; radial air swirlers.]

| Run | Simulated flight condition | Inlet air conditions | | | | Combustor operating conditions | | | | |
|---|---|---|---|---|---|---|---|---|---|---|
| | | Total pressure, $N/cm^2$ abs | Total temperature K | Airflow, kg/sec | Diffuser inlet Mach number, $M_3$ | Reference velocity, m/sec | Fuel-air ratio | Average outlet temperature, K | Inlet fuel temperature, K | Fuel nozzle differential pressure, $N/cm^2$ |
| 324 | Takeoff | 62.3 | 587 | 50.5 | 0.249 | 31.9 | 0.0252 | 1476 | 292 | 213.6/229.5 |
| 223 | Mach 2.7 cruise | 41.4 | 849 | 33.8 | .310 | 46.4 | .0182 | 1462 | 293 | 60.5/43.4 |
| 319 | Mach 3.0 cruise | 61.6 | 896 | 49.0 | .312 | 47.7 | .0173 | 1478 | 296 | 91.4/97.5 |

| Run | Simulated flight condition | Combustor performance characteristics | | | | | |
|---|---|---|---|---|---|---|---|
| | | Pattern factor, $\bar{\delta}$ | Stator factor, $\bar{\delta}_s$ | Rotor factor, $\bar{\delta}_r$ | Combustor average temperature rise, K | Combustor pressure loss, percent | Combustion efficiency, $\eta_c$, percent |
| 324 | Takeoff | 0.397 | 0.382 | 0.014 | 889 | 5.79 | 102.9 |
| 223 | Mach 2.7 cruise | .202 | .267 | .056 | 613 | 8.25 | 100.1 |
| 319 | Mach 3.0 cruise | .147 | .215 | .097 | 582 | 8.33 | 101.1 |

TABLE V. - DOUBLE-ANNULAR RAM-INDUCTION COMBUSTOR DIMENSIONS AND SPECIFICATIONS

| | |
|---|---|
| Length: | |
| Compressor exit to turbine inlet, cm | 51.5 |
| Fuel nozzle face to turbine inlet, cm | 30.5 |
| Diameter: | |
| Inlet outside diameter, cm | 80.77 |
| Inlet inside diameter, cm | 71.1 |
| Outlet outside diameter, cm | 89.9 |
| Outlet inside diameter, cm | 69.9 |
| Shroud: | |
| Outside diameter, cm | 94.2 |
| Inside diameter, cm | 57.2 |
| Reference area (between shrouds), $cm^2$ | 4270 |
| Diffuser inlet area, $cm^2$ | 1177 |
| Open hole area (including cooling), $cm^2$ | 1571 |
| Flow spreader inlet area: | |
| Outside diameter passage, $cm^2$ | 348 |
| Center passage, $cm^2$ | 785 |
| Inside diameter passage, $cm^2$ | 339 |
| Exit area, $cm^2$ | 2503 |
| Number of fuel nozzles and swirlers | 64 |
| Number of diffuser struts | 16 |
| Number of ram-induction scoop | 256 |
| Number of primary zone scoop rows | 1 |
| Number of secondary zone scoop rows | 1 |
| Ratio length to annulus height: | |
| Outer annulus | 4.8 |
| Inner annulus | 3.9 |

TABLE VI. - SCOOP AREAS[a] AND SIZES FOR DOUBLE-ANNULAR RAM-INDUCTION COMBUSTOR[b]

| Type of scoop | Discharge area, $cm^2$ | Length, cm | Width, cm |
|---|---|---|---|
| Outer liner primary | 122.73 | 1.979 | 3.835 |
| Outer liner secondary | 218.64 | 2.637 | 2.591 |
| Outer center shroud primary | 122.85 | 1.981 | 1.938 |
| Outer center shroud secondary | 109.03 | 1.295 | 3.407 |
| Inner center shroud primary | 122.85 | 1.981 | 1.938 |
| Inner center shroud secondary | 109.03 | 1.295 | 3.407 |
| Inner liner primary | 122.35 | 2.07 | 1.847 |
| Inner liner secondary | 219.25 | 3.31 | 2.07 |

[a]All areas are actual area for full annulus.
[b]See fig. 1.

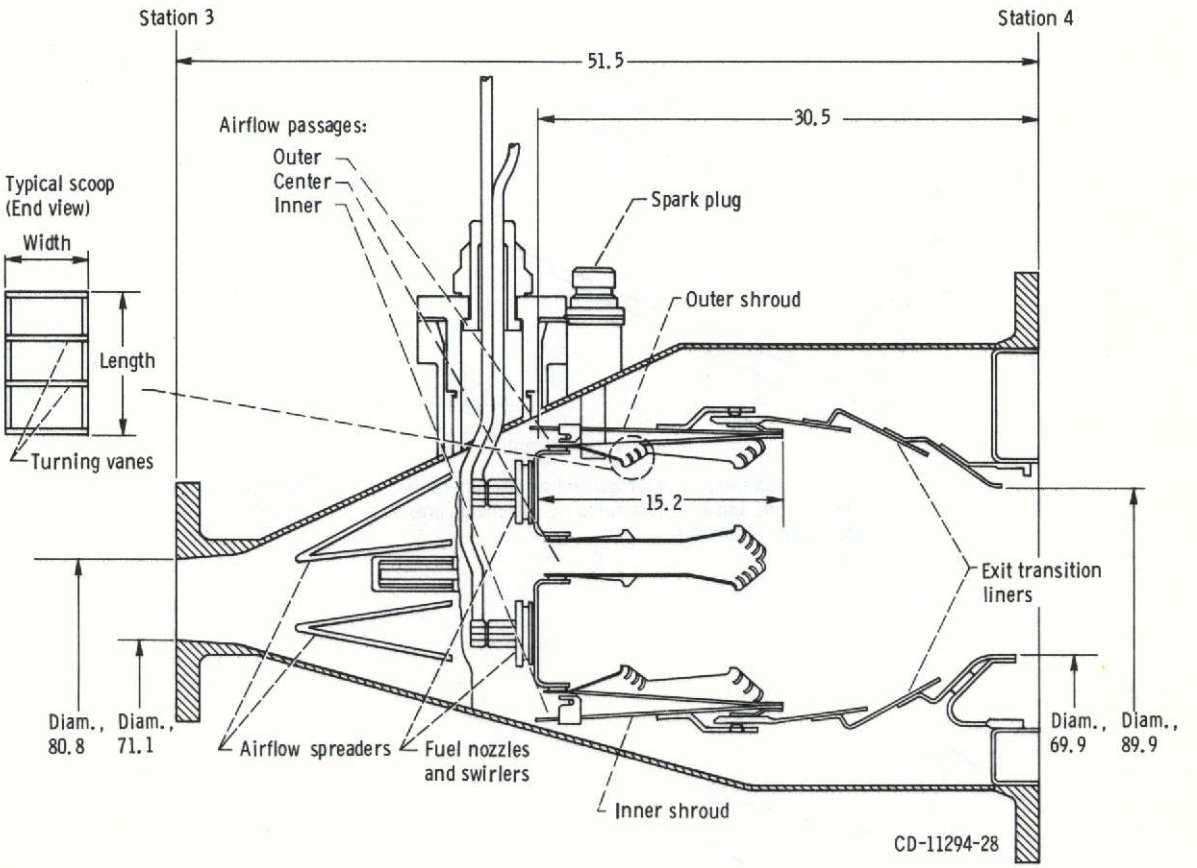


Figure 1. - Cross section of double-annular ram-induction combustor. (All dimensions are in cm.)

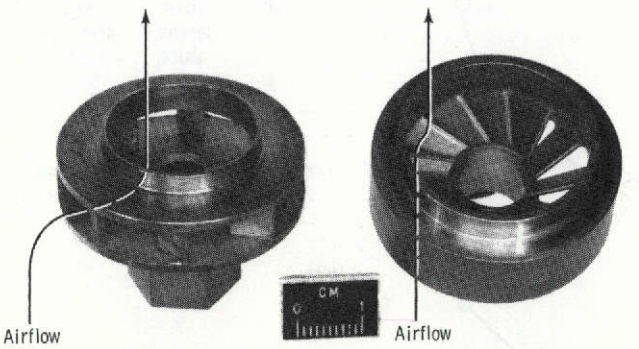


Figure 2. - Detail of the radial inflow and axial flow air switches.

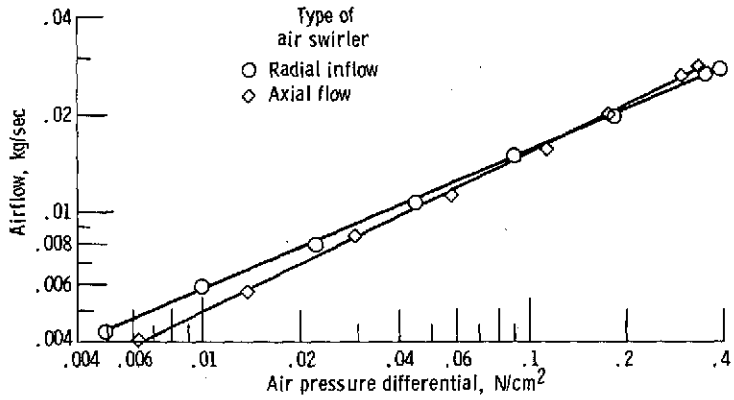


Figure 3. - Comparison of airflow and swirler differential pressure for the radial-inflow and axial-flow swirlers. Discharge pressure, 9.9 newtons per square centimeter.

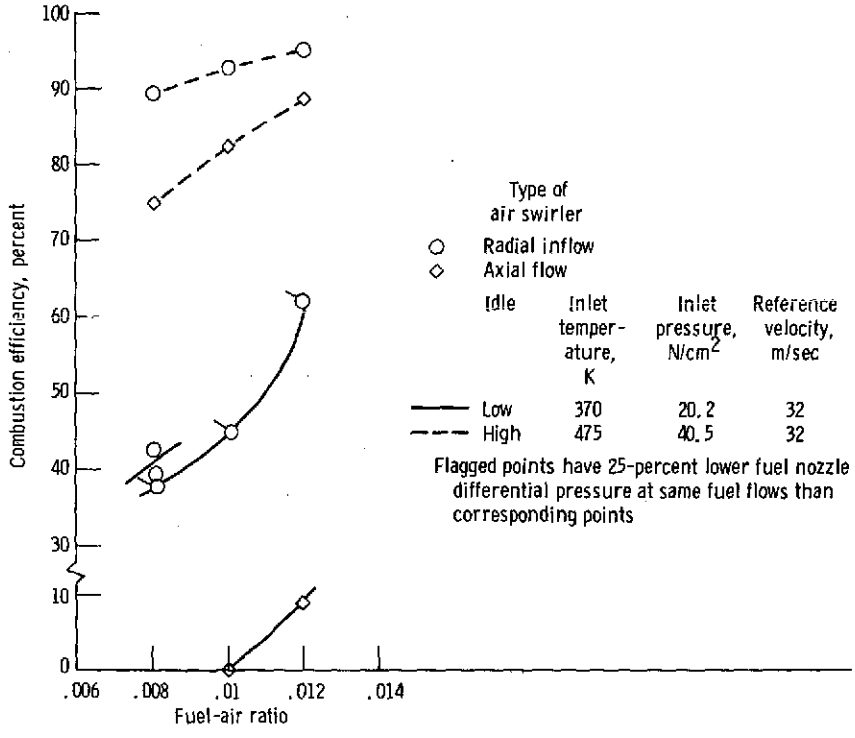


Figure 4. - Combustion efficiency as function of fuel-air ratio comparing radial inflow and axial flow air swirlers. Fuel nozzle spray angle, 60°.

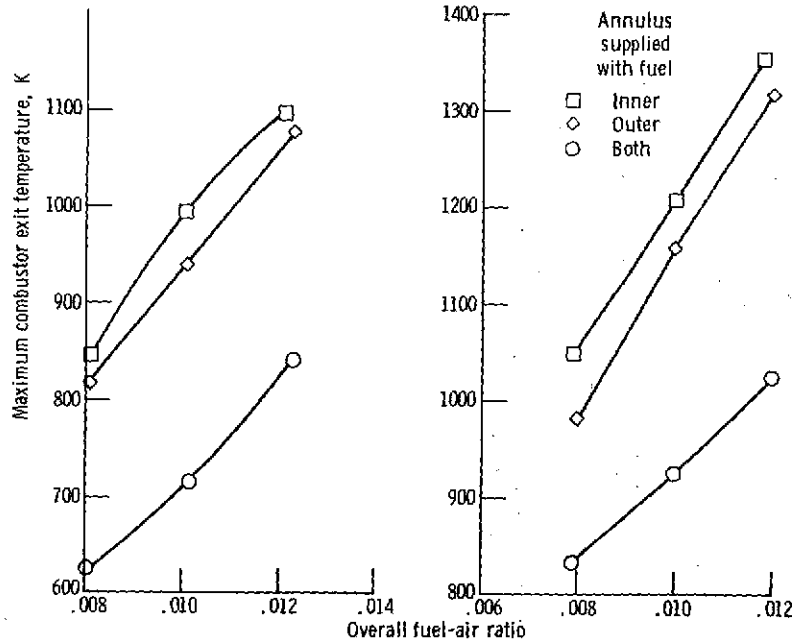


(a) Low idle; inlet total pressure, 20.2 newtons per square centimeter; inlet temperature, 370 K; reference velocity, 32 meters per second.

(b) High idle; inlet total pressure, 40.5 newtons per square centimeter; inlet temperature, 475 K; reference velocity, 32 meters per second.

Figure 5. - Maximum combustor exit temperature as function of fuel-air ratio showing effect of radial fuel staging at both low and high idle. Radial-inflow air swirlers; fuel nozzles H3.

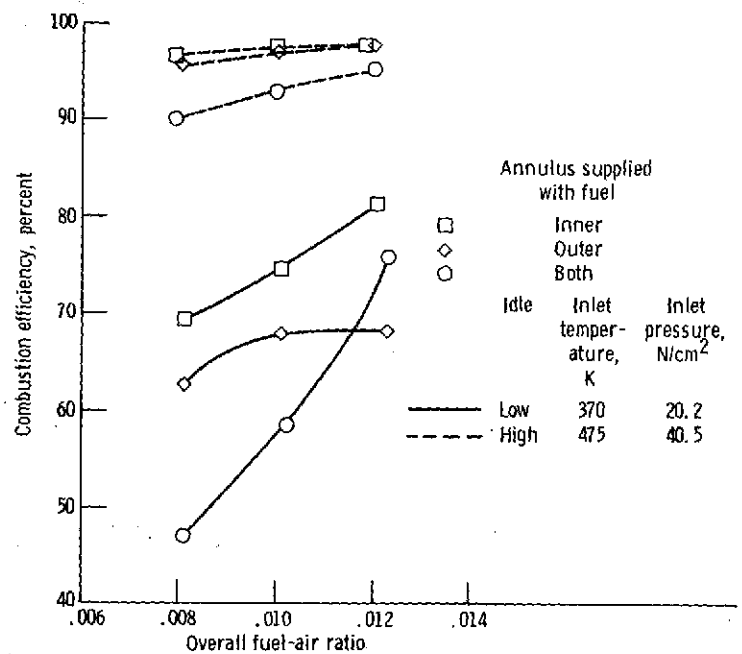


Figure 6. - Combustion efficiency as function of fuel-air ratio showing effect of radial fuel staging at low and high idle. Fuel nozzles, H3; reference velocity, 32 meters per second.

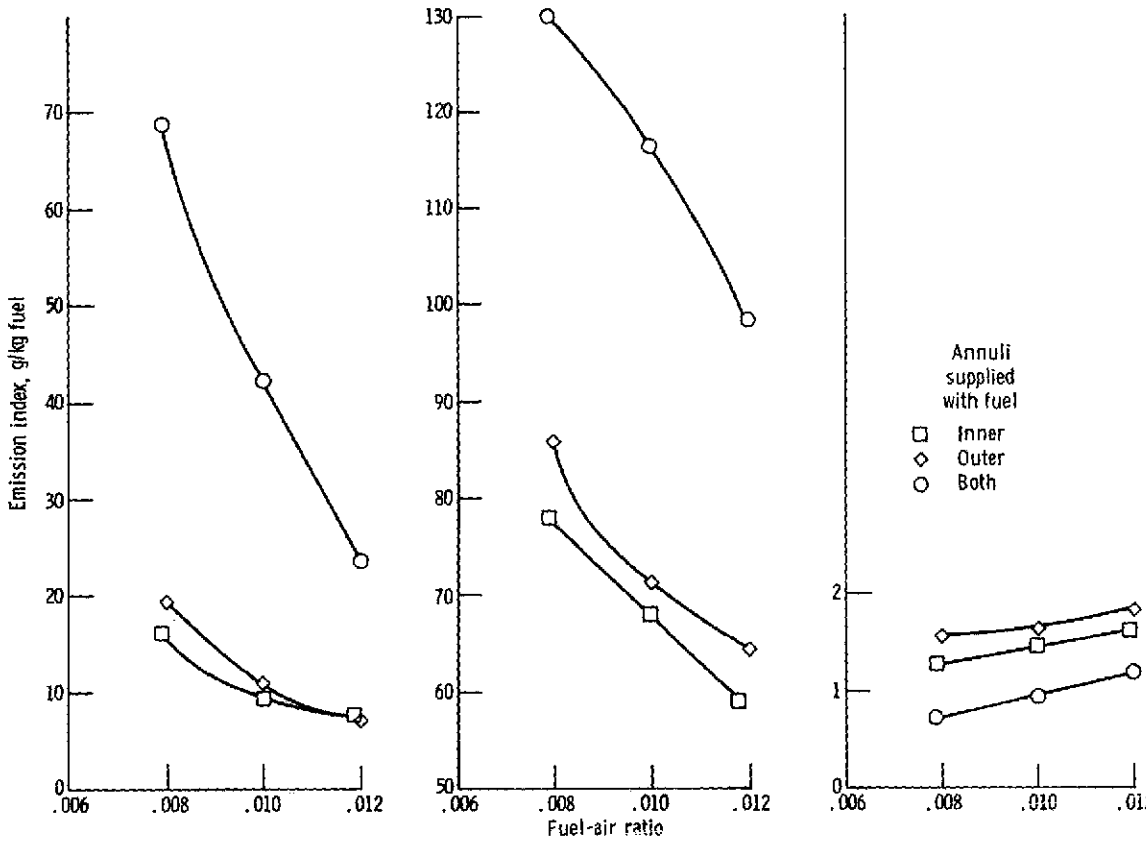


(a) Hydrocarbon. (b) Carbon monoxide. (c) Oxides of nitrogen (fuel nozzle H3).

Figure 7. - Emissions index as function of fuel-air ratio. High idle conditions: inlet total pressure, 40.5 newtons per square centimeter; inlet temperature, 475 K; reference velocity, 32 meters per second.

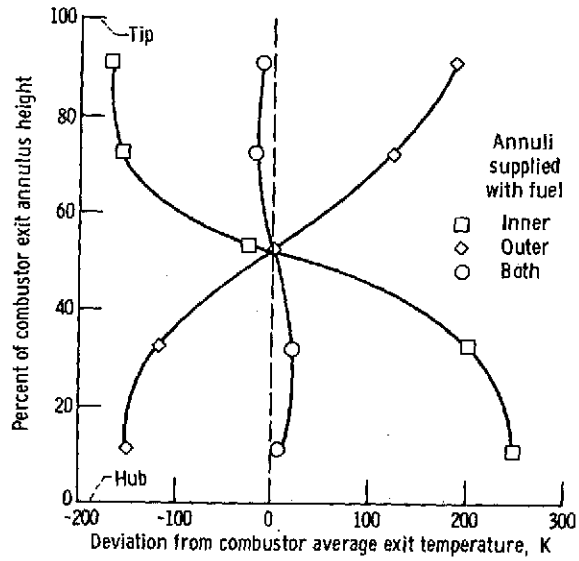


Figure 8. - Variation of exit average radial temperature profile with radial fuel staging. High idle conditions; total pressure, 40.5 newtons per square centimeter; inlet temperature, 475 K; reference velocity, 32 meters per second; fuel-air ratio, 0.012.

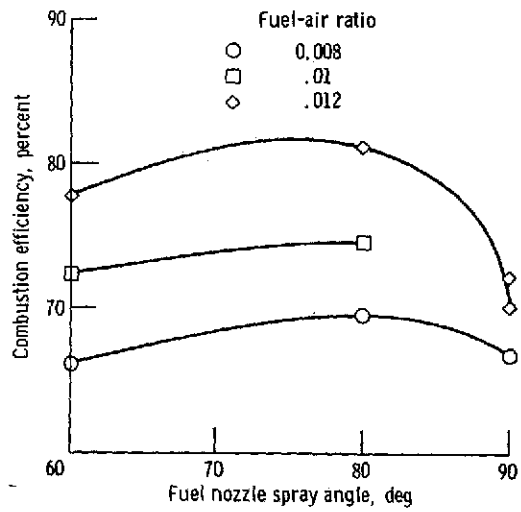


Figure 9. - Combustion efficiency as function of fuel nozzle spray angle showing effect of fuel-air ratio. Low idle conditions: inlet total pressure, 20.2 newtons per square centimeter; inlet temperature, 370 K; reference velocity, 32 meters per second. Radial-inflow swirlers; fuel to inner annulus only.

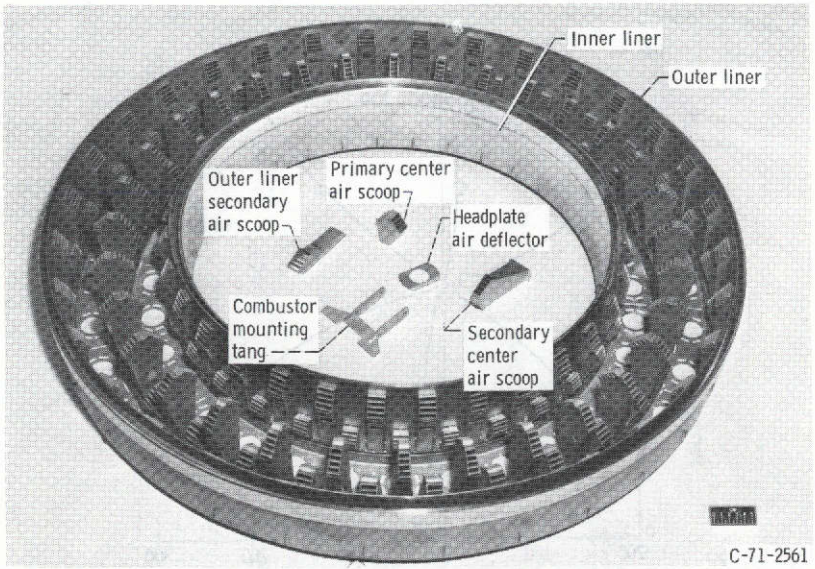


(a) Viewed from downstream (fuel nozzles, headplate, air deflectors, and transition liners removed).

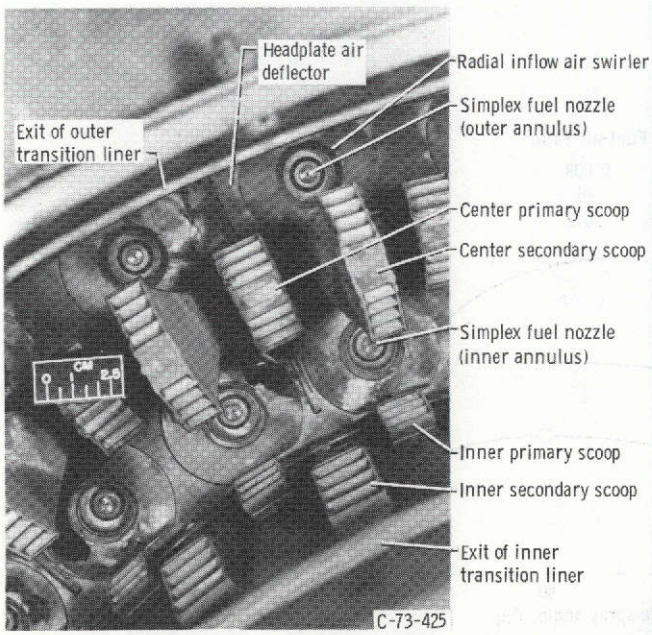


(b) Closeup.

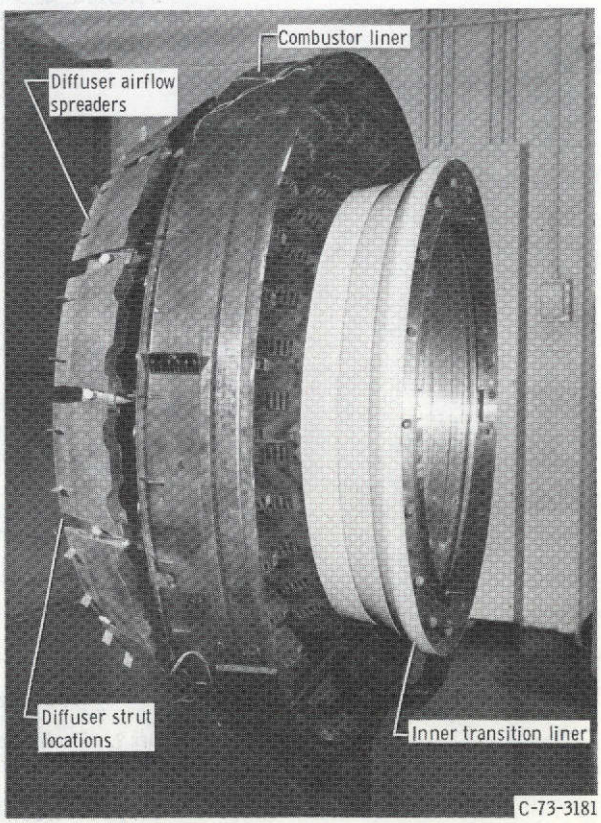


(c) Side view (outer transition liner removed).

Figure 10. - Double annular ram-induction combustor.

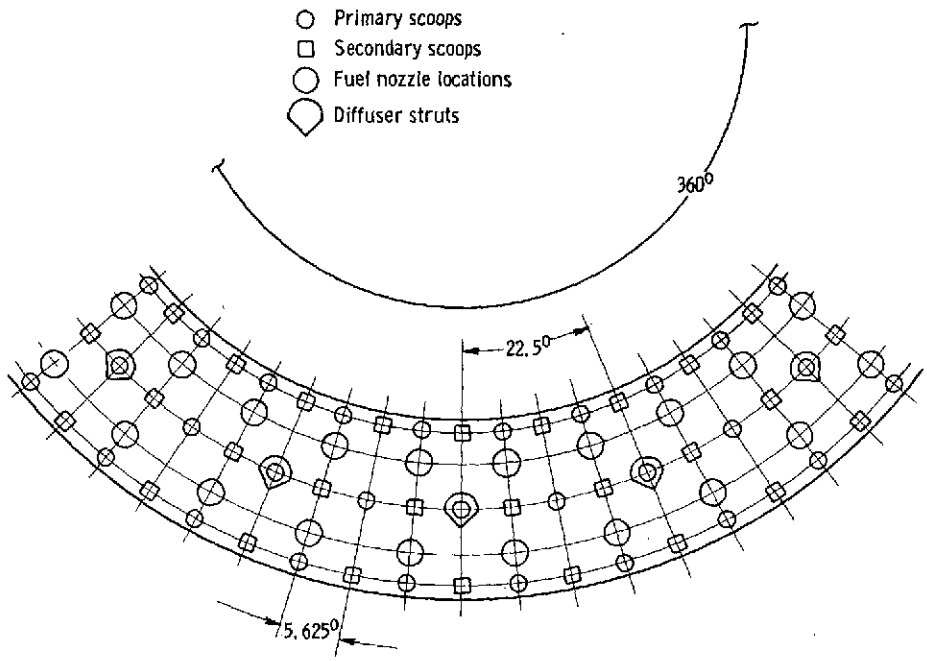


Figure 11. - Circumferential arrangement of combustor scoops and fuel nozzles.

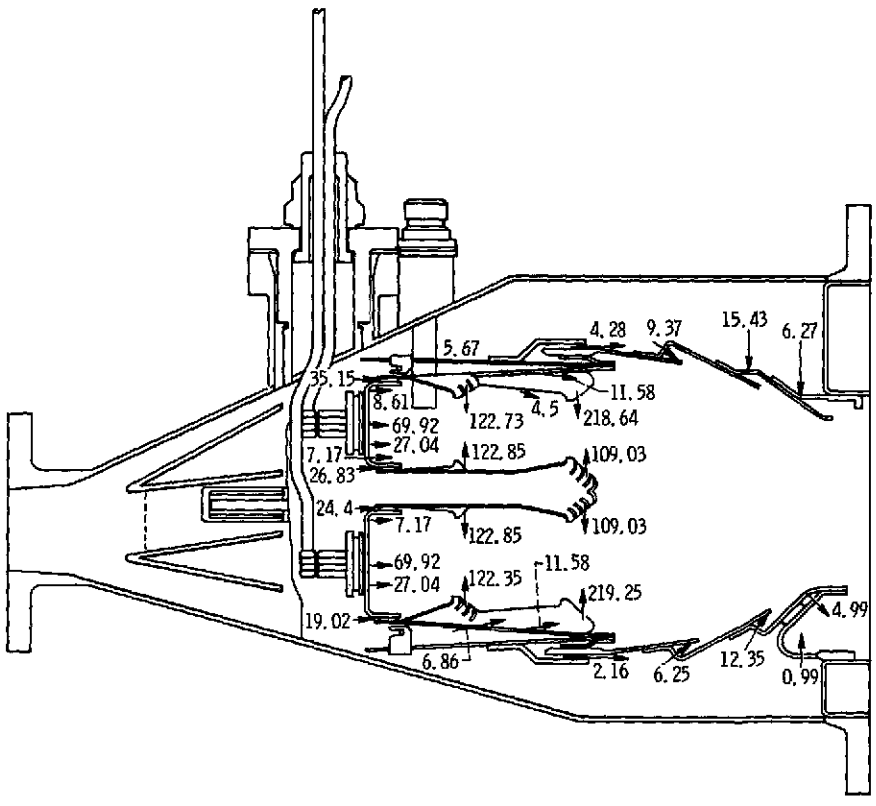


Figure 12. - Effective flow area distribution for double-annular ram-induction combustor. Swirler discharge coefficient, 0.50; hole discharge coefficient, 0.62; scoops and slot discharge coefficient, 1.00; total area (effective), 1571 square centimeters. (All areas are based on a full annulus with units of $cm^2$.)